Received August 2000
Revised February 2001
Accepted February 2001

A comparative study on the performance of two time stepping schemes for convection in a fluid saturated porous medium

P. Nithiarasu
Institute for Numerical Methods in Engineering, Department of Civil Engineering, University of Wales Swansea, Swansea, UK

Keywords *Finite element method, Semi-implicit, Porous media, Convection*

Abstract *A comparative study has been carried out to investigate the performance of two different time stepping schemes for convective heat transfer and flow in a fluid saturated porous medium. Both the schemes are based on the velocity correction procedure. The first scheme is a semi-implicit one in which the linear and non-linear porous medium terms of the momentum equation are treated implicitly but solution of the simultaneous equation system is avoided by lumping the mass. The second procedure (quasi-implicit) treats the porous medium and viscous terms implicitly and a simultaneous equation system is constructed to solve the equations of momentum conservation. Two numerical examples have been considered and both the schemes are tested for various parameters governing the flow and heat transfer in these problems. Results show that, at smaller Rayleigh numbers and on fine meshes, the quasi-implicit scheme gives faster convergence to steady state in both Darcy and non-Darcy regimes than that of the semi-implicit scheme. At higher Rayleigh numbers, the semi-implicit scheme is faster in the Darcy regime. Also, the semi-implicit scheme is faster than that of the quasi-implicit scheme on a coarse mesh used in this study. In general both the schemes predict transient cyclic developments well.*

Nomenclature

c_p = specific heat
Da = Darcy number (κ/L^2)
g = acceleration due to gravity
J = viscosity ratio (μ_{eff}/μ_f)
k = average thermal conductivity ($\epsilon k_f + (1-\epsilon)k_s$)
k^* = conductivity ratio (k/k_f)
L = characteristic dimension
$\mathbf{N}$ = shape functions
Nu = average Nusselt number
p = pressure
Pr = Prandtl number (ν/α)
Ra = Rayleigh number ($g\beta\Delta TL^3/\nu\alpha$)
T = temperature
t = time
u_i = velocity components
u_1 = velocity component in the horizontal direction
u_2 = velocity component in the vertical direction
$|\mathbf{V}|$ = magnitude of the velocity vector
x_i = coordinate axes

Superscript
n = nth time iteration

Subscripts
f = fluid
s = solid

Greek symbols
α = thermal diffusivity
β = coefficient of thermal expansion
ϵ = porosity
κ = permeability
ν = kinematic viscosity
ρ = density
σ = ratio of heat capacities, $(\epsilon(\rho c_p)_f + (1-\epsilon(\rho c_p)_s)/(\rho c_p)_f)$

International Journal of Numerical Methods for Heat & Fluid Flow, Vol. 11 No. 4, 2001, pp. 308-328.

1. Introduction

Flow through porous media has been a subject of intense research in the last few decades due to many applications such as underground fluid flow, building and other insulations, nuclear waste disposal, alloy solidification etc. There are many numerical studies available in the literature to solve flow through porous media. However, identifying new and accurate numerical solution techniques is essential in order to make the solvers more efficient. Both finite element and finite volume techniques have been employed by researchers in the porous medium flow calculations but, in this study, only the finite element method is adopted. However, the algorithms discussed here can also be implemented by using finite volume techniques.

The finite element method has been adopted by many authors in the past to solve fluid flow through porous media (Hickox and Gartling, 1985; Nishimura *et al.*, 1986; Rajamani *et al.*, 1990; 1995; Misra and Sarkar, 1995; Gartling *et al.*, 1996). The majority of these studies use steady state flow equations to solve the porous medium problems and use standard Galerkin discretization.

Although the velocity correction algorithm for single phase flows was initiated in the late 1960s by Chorin (1968) and developed by others (Comini and Del Giudice, 1982; Donea *et al.*, 1982; Ramaswamy, 1988, 1993; Ramaswamy *et al.*, 1992; Zienkiewicz and Codina, 1995; Zienkiewicz *et al.*, 1999), it was not used in the porous medium flow analysis until 1996. This approach was first introduced for the generalised porous medium applications by Nithiarasu *et al.* (1996), in which a quasi-implicit (*QI*) procedure (sometimes called semi-implicit) was employed. Later, the *QI* scheme was successfully applied to many porous medium applications (Sai *et al.*, 1997; Nithiarasu *et al.*,1997, 1998a, 1998b, 1999).

An alternative form of the velocity correction procedure for porous medium flows was suggested by Nithiarasu and Ravindran (1998), in which a semi-implicit (*SI*) form was adopted, and was aimed to remove the simultaneous equation system when solving the equations of momentum conservation. Such a scheme cannot be constructed as a direct extension of Navier-Stokes solvers due to extra porous medium terms in the momentum equations. Recently the *SI* scheme has been successfully applied to anisotropic porous medium flows (Nithiarasu *et al.*, 2000) and to domains with both porous medium and free fluids (Massarotti *et al.*, 2000).

Although earlier papers give the implementation details of the above schemes, a comparative study was not carried out on the performance of these schemes. In this paper such an investigation is conducted to evaluate the relative performance and the advantages and disadvantages of the above schemes.

2. Governing equations

The properties of the medium considered in this study except the density are assumed to be constant and the density variation is incorporated through Boussinesq approximation. The generalised set of non-dimensional governing

equations for the buoyancy driven flow and heat transfer with uniform porosity are given as:

Continuity equation

$$\frac{\partial u_i}{\partial x_i} = 0 \tag{1}$$

Momentum equation

$$\frac{1}{\epsilon}\frac{\partial u_i}{\partial t} + \frac{1}{\epsilon^2}u_j\frac{\partial u_i}{\partial x_j} = -\frac{\partial p}{\partial x_i} + \frac{JPr}{\epsilon}\left[\frac{\partial^2 u_i}{\partial x_i^2}\right] - \frac{Pr}{Da}u_i - \frac{1.75}{\sqrt{150}}\frac{|\mathbf{V}|}{\sqrt{Da}}\frac{u_i}{\epsilon^{3/2}} + \gamma_i RaPrT \tag{2}$$

Energy equation

$$\sigma\frac{\partial T}{\partial t} + u_i\frac{\partial T}{\partial x_i} = k^*\left(\frac{\partial^2 T}{\partial x_i^2}\right) \tag{3}$$

The detailed derivation of the governing equations is discussed elsewhere (Vafai and Tien, 1981; Hsu and Cheng, 1990); Nithiarasu *et al.*, 1997). In the momentum equations (equation 2), the non-linear matrix drag is incorporated through Ergun's correlation (Ergun, 1952; Nithiarasu *et al.*, 1997); u_i are volume averaged velocity components; ϵ the porosity of the medium and assumed to be uniform throughout the domain; Pr the Prandtl number; Ra the fluid Rayleigh number; Da the Darcy number; σ the ratio of heat capacities; γ_i a vector equal to unity in the vertical direction and zero in the horizontal direction and T the non-dimensional temperature.

In the momentum equations (equation 2), J is the viscosity ratio. This ratio and the conductivity ratio k^* in the energy equation are taken as unity in the present study for the sake of simplicity. It is also assumed that the thermal equilibrium between the phases exists.

3. Solution procedures

In the present study, the velocity correction procedure is employed. The method originally introduced in the finite difference context by Chorin (1968) attracted many finite element researchers later. Some finite element implementations of velocity correction procedure can be found in Comini and Del Giudice (1982); Donea *et al.* (1982); Ramaswamy (1988, 1993); Ramaswamy *et al.* (1992); Zienkiewicz and Codina (1995); Zienkiewicz *et al.* (1999). Similar schemes developed to solve the porous medium equations are discussed here. The four essential steps are:

(1) solving the momentum equations without pressure terms;

(2) calculation of pressure from the Poisson equation;

(3) correcting the velocities; and

(4) calculation of temperature field from the energy equation.

The main advantage of using the velocity correction procedure is due to equal order interpolation for pressure and velocity, which reduces the complexity and CPU time. At step 1, the intermediate vertical velocity component can be calculated by two different schemes, as given below. Steps 2 and 3 are identical in both the *SI* and *QI* schemes. However, at step 4, the diffusion terms of the energy equations are treated implicitly in the *QI* scheme and explicitly in the *SI* scheme.

Semi-implicit (SI) scheme. As mentioned before, here the porous medium terms are treated implicitly and the temporal discretization of the momentum equation can be written as (Nithiarasu and Ravindran, 1998):

$$\frac{\tilde{u}_i^{n+1} - u_i^n}{\epsilon \Delta t} = -\frac{1}{\epsilon^2}\left[u_j \frac{\partial u_i}{\partial x_j}\right]^n + \frac{PrJ}{\epsilon}\left(\frac{\partial^2 u_i}{\partial x_i^2}\right)^n + \left[-\frac{Pr}{Da}\tilde{u}_i - \frac{1.75}{\sqrt{150}}\frac{|\overline{V}|}{\sqrt{Da}}\frac{\tilde{u}_i}{\epsilon^{3/2}}\right]^{n+1} + \gamma_i RaPrT^n \tag{4}$$

where ˜ indicates intermediate velocity components. Note that the pressure terms are completely removed from the momentum equations. The above equation can be rearranged and the final matrix form of the discretized equation by using the Galerkin spatial approximation is given as:

$$[\mathbf{M}]\{\tilde{\mathbf{u}}_\mathbf{i}^{n+1}\} = C^{-1}\left\{\frac{1}{\epsilon}[\mathbf{M}]\{\mathbf{u_i}\} + \Delta t[\mathbf{K}]\{\mathbf{u_i}\} - \Delta t[\mathbf{A}]\{\mathbf{u_i}\} + \Delta t\{\mathbf{F}\} + \gamma_i \Delta t RaPr[\mathbf{M}]\{\mathbf{T}\}\right\}^n \tag{5}$$

where $\{\mathbf{F}\}$ is the boundary terms from viscous contribution; C is a coefficient and, for a constant porosity medium, it is given as

$$C = \left[\frac{1}{\epsilon} + \Delta t\frac{Pr}{Da} + \Delta t\frac{1.75}{\sqrt{150}}\frac{|\mathbf{V}|}{\sqrt{Da}}\frac{1}{\epsilon^{3/2}}\right] \tag{6}$$

In equation 5, the matrices are

$$\mathbf{M} = \int_\Omega \mathbf{N}^T\mathbf{N}d\Omega; \quad \mathbf{K} = \frac{JPr}{\epsilon}\int_\Omega \frac{\partial \mathbf{N}^T}{\partial x_i}\frac{\partial \mathbf{N}}{\partial x_i}d\Omega; \mathbf{A} = \frac{1}{\epsilon^2}\left[\int_\Omega \mathbf{N}^T\mathbf{N}\mathbf{u_j}^n\frac{\partial \mathbf{N}^T}{\partial x_j}d\Omega\right] \tag{7}$$

In equation 5, the mass matrix **M** is lumped and the solution is directly updated at each time step and no simultaneous equations are solved at the intermediate velocity calculation stage.

Quasi-implicit (QI) scheme. In the quasi-implicit solution, in addition to the porous medium terms, the viscous terms are also treated implicitly and a simultaneous equation set is solved. The temporal discretization of the momentum transport can be written as (Nithiarasu *et al.*, 1996):

$$\frac{\tilde{u}_i^{n+1} - u_i^n}{\epsilon \Delta t} = -\frac{3}{2\epsilon^2}\left[u_j \frac{\partial u_i}{\partial x_j}\right]^n + \frac{1}{2\epsilon^2}\left[u_j \frac{\partial u_i}{\partial x_j}\right]^{n-1} + \left[\frac{PrJ}{\epsilon}\left(\frac{\partial^2 \tilde{u}_i}{\partial x_i^2}\right) - \frac{Pr}{Da}\tilde{u}_i - \frac{1.75}{\sqrt{150}}\frac{|\overline{V}|}{\sqrt{Da}}\frac{\tilde{u}_i}{\epsilon^{3/2}}\right]^{n+1} + \gamma_i RaPrT^n \tag{8}$$

Here, the porous medium terms are treated implicitly in addition to the viscous terms. Note that the Adams-Bashforth type of time marching is adopted for convective terms in the above equation, as recommended by Ramaswamy *et al.* (1992). The Galerkin's finite element method is used for the spatial discretization of the above equation. The final matrix form of the discretized equation is given as

$$\left\{\frac{1}{\epsilon}[\mathbf{M}] + \Delta t[\mathbf{K}] + \Delta t[\mathbf{D_1}] + \Delta t[\mathbf{D_2}]\right\}\tilde{\mathbf{u}}_\mathbf{i} = \frac{1}{\epsilon}[\mathbf{M}]\mathbf{u}_\mathbf{i}^\mathbf{n} + \Delta t\{\{\mathbf{F}\} - [\mathbf{A_1}]\mathbf{u}_\mathbf{i}^\mathbf{n} + [\mathbf{A_2}]\mathbf{u}_\mathbf{i}^{\mathbf{n-1}}\} + \Delta t\gamma_i[\mathbf{M}]RaPr\mathbf{T}^\mathbf{n} \tag{9}$$

where

$$\mathbf{D_1} = \frac{Pr}{Da}[\mathbf{M}]; \quad \mathbf{D_2} = \frac{1.75}{\sqrt{150}}\frac{(|\mathbf{V}|)^n}{\sqrt{Da}}\frac{1}{\epsilon^{3/2}}[\mathbf{M}]$$
$$\mathbf{A_1} = \frac{1}{\epsilon^2}\left[\frac{3}{2}\int_\Omega \mathbf{N}^T\mathbf{N}\mathbf{u_j}^n\frac{\partial \mathbf{N}^T}{\partial x_j}d\Omega\right]; \ \mathbf{A_2} = \frac{1}{\epsilon^2}\left[\frac{1}{2}\int_\Omega \mathbf{N}^T\mathbf{N}\mathbf{u_j}^{n-1}\frac{\partial \mathbf{N}^T}{\partial x_j}d\Omega\right] \tag{10}$$

It should be noted that matrices $\mathbf{D_1}$ and $\mathbf{D_2}$ are introduced to the left-hand side as part of implicit terms, as these matrices can impose time step restrictions if treated explicitly. However, other alternatives such as introduction of C, as in the *SI* scheme, could be possible. Such an alternative is not investigated in this paper. Integration of the above quantities for linear triangular elements is simple and is discussed in many textbooks (Zienkiewicz and Taylor, 2000).

In both the *SI* and *QI* schemes, the other three steps follow the standard procedure discussed in many references (Nithiarasu *et al.*, 1996, 1997, 1998a, 1998b, 2000; Nithiarasu and Ravindran, 1998; Massarotti *et al.*, 2000). The pressure Poisson equation is derived by satisfying the conservation of mass and solved implicitly in both the *SI* and *QI* schemes. At the velocity correction

stage, the mass matrices are lumped in both these procedures. However, as mentioned before, the temperature calculation in the *SI* scheme differs from that of the *QI* scheme. In the former, the temperature is calculated explicitly with lumped mass matrices and, in the latter procedure, viscous terms of the energy equations are treated implicitly and the linear simultaneous equation system is solved.

In both the schemes, the direct, banded, Gaussian elimination procedure has been employed to solve any linear simultaneous system of equations. In the *SI* scheme, only step 2 is employed in which the simultaneous equation system is solved to evaluate pressure implicitly. In the *QI* scheme the simultaneous system of equations is solved at steps 1, 2 and 4.

The time marching of the four steps is continued until the nodal velocities, pressure and temperature approach steady state within a specified difference in the value of the variable between successive time steps. The maximum nodal value of this difference has been set as 10^{-7} for velocity and temperature fields, i.e:

$$(u_i^{n+1} - u_i^n)_{\max} < 10^{-7}; \quad (T^{n+1} - T^n)_{\max} < 10^{-7} \tag{11}$$

where n indicates the nth time step. The above values will reduce the residual values to small quantities. Since equation (11) is considered as the convergence criterion, no fixed value of allowable residual value is used. However, in all calculations it was ensured that maximum nodal values

$$\left(\frac{u_i^{n+1} - u_i^n}{\Delta t}\right)_{\max} \tag{12}$$

and

$$\left(\frac{T^{n+1} - T^n}{\Delta t}\right)_{\max} \tag{13}$$

are smaller than 0.05. Note that the above values are the maximum among the nodal values, not averaged quantities.

4. Results and discussion

To carry out a performance study on the *QI* and *SI* schemes discussed above, a model, benchmark problem of buoyancy driven flow in a square cavity filled with a fluid saturated porous medium is considered first. Figure 1 shows the problem domain and boundary conditions. All the walls are assumed to be non-slip. Constant temperature is assumed on vertical walls and the left wall temperature is higher than that of the right. Both the horizontal walls are assumed to be insulated.

The first finite element mesh used is 51×51 in size and non-uniform (5,000 elements). First point from any wall is placed at a non-dimensional distance of 0.005. This mesh was proved to be a converged mesh for the Rayleigh and

Darcy number range considered in this study (Nithiarasu *et al.*, 1999). In order to test the schemes on a non-converged, coarse mesh, a uniform grid of size 31 $\times$ 31 (1,800 elements) is also used in this study. The elements used throughout the paper are the linear triangles.

The analysis is carried out for two different Darcy numbers , $Da = 10^{-6}$ in the Darcy flow regime and $Da = 10^{-2}$ in the non-Darcy flow regime. The fluid Rayleigh numbers of 10^8, 10^9 and 5×10^9 are considered in the Darcy flow regime and 10^4, 10^5 and 5×10^5 have been used in the non-Darcy flow regime. The porosity is assumed to be constant throughout the domain and a fixed value of 0.6 is assumed. The Prandtl number is assumed to be equal to unity. For each case a highest (approximately) time step value accepted by the schemes is employed.

Since the qualitative results of this problem were discussed in detail in many earlier publications, the present paper concentrates only on the CPU time, convergence history and average Nusselt number distribution.

Table I shows the CPU time taken by both the schemes to reach steady state. As we can see, at smaller Rayleigh numbers, on the fine mesh (10^8 in the Darcy regime and 10^4 in the non-Darcy regime) the *QI* scheme is very efficient. The time taken by the *QI* scheme here is very short compared with that of the *SI* scheme at these Rayleigh numbers. However, in the Darcy regime, at higher Rayleigh numbers, surprisingly the CPU time taken by the *SI* scheme is much shorter than that of the *QI* scheme. An even more surprising result is that the *SI* scheme took much less CPU at higher Rayleigh numbers than that at 10^8 and 10^4 in the Darcy and non-Darcy regimes respectively. On the other hand, in the non-Darcy regime the *QI* scheme has taken shorter CPU time than that of the *SI* scheme.

Table I also shows the CPU time taken by both schemes on a coarse 31 $\times$ 31, uniform mesh. As can be seen, the *SI* scheme has performed better than that of the *QI* scheme on this grid. The performance of the *SI* scheme is good not only on the CPU time taken but also on giving a converged solution for all the Darcy and Rayleigh numbers considered. On the other hand, the *QI* scheme has taken many CPU seconds and also has not given a converged solution in the Darcy

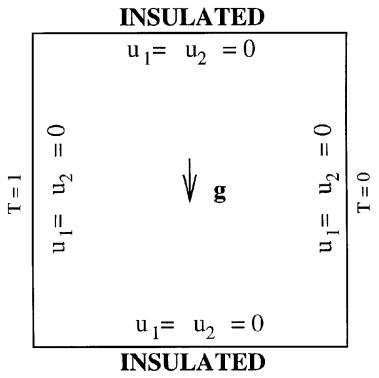

Figure 1.
Buoyancy driven flow in a fluid saturated porous medium. Geometry and boundary conditions

flow regime at Ra = 5×10^9. Thus it appears that the *SI* scheme is suitable for problems where a coarse mesh solution is essential.

The time steps used in each case are also given in Table I (in periphrases). On the fine mesh, the *SI* scheme accepts time-steps generally smaller than that of the *QI* scheme for the Darcy and Rayleigh numbers considered. However, this is not true on the coarse mesh where the *SI* scheme accepts higher time steps than that of the *QI* scheme at higher Rayleigh numbers.

The above discussion shows that the *QI* scheme is not always more efficient than that of the *SI* scheme. However, the *QI* scheme was proved to be more efficient than that of the *SI* scheme for single-phase flows in the past (Ramaswamy *et al.*, 1992).

Figures 2-4 show the convergence history of the variables u_1, u_2 and T for both the schemes on the fine mesh. As expected, at a smaller Rayleigh number of 10^8 in the Darcy regime (Figure 2), the *QI* scheme converges rapidly within 150 time steps. However, the *SI* scheme took more than 20,000 time steps to converge at these Rayleigh and Darcy numbers. In Figure 3, at a higher Rayleigh number of 10^9, the number of time steps taken by the *SI* scheme to reach steady state is much smaller than that at 10^8. Here, as was seen, the total number of time steps taken by both the *SI* and *QI* schemes is very close and therefore obviously the *QI* scheme requires more CPU time. In Figure 4 however, there is a large difference in number of time steps taken by these schemes to reach steady state. Thus in the non-Darcy regime, the *QI* scheme accepts much higher time steps on the fine mesh and reaches steady state faster than that of the *SI* scheme.

The convergence history of the variables on the coarse mesh is not given here for the sake of brevity. However, it can be seen from Table I that the *SI* scheme generally is faster on the coarse mesh than that of the *QI* scheme.

Da	*Ra*	*SI* (Fine grid)	*QI* (Fine grid)	*SI* (Coarse grid)	*QI* (Coarse grid)
10^{-6}	10^8	17,836 (8×10^{-6})	216 (5×10^{-3})	232 (2×10^{-4})	471 (6×10^{-3})
10^{-6}	10^9	8,894 (8×10^{-6})	14,692 (2×10^{-5})	206 (1×10^{-4})	2,618 (3×10^{-5})
10^{-6}	5×10^9	14,106 (8×10^{-6})	78,194 (2×10^{-6})	985 (1×10^{-5})	not converged
10^{-2}	10^4	23,173 (8×10^{-6})	277 (5×10^{-3})	312 (2×10^{-4})	40 (1×10^{-2})
10^{-2}	10^5	18,210 (8×10^{-6})	1,597 (5×10^{-4})	233 (2×10^{-4})	430 (5×10^{-4})
10^{-2}	5×10^5	14,871 (8×10^{-6})	7,940 (7×10^{-5})	358 (1×10^{-4})	1,901 (8×10^{-5})

Note: The time steps used in each case are given in parentheses

Table I. Comparison of CPU time in seconds on a Pentium 166. Buoyancy driven flow in a square cavity. Fine mesh size: 51 × 51 (non-uniform). Coarse mesh size: 31 × 31 (uniform)

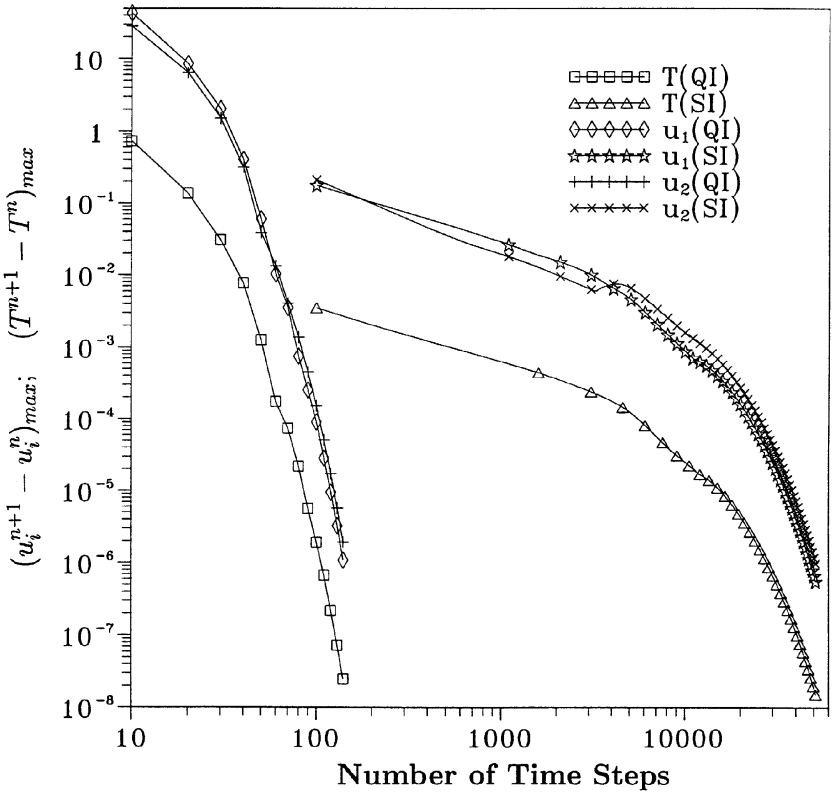

Figure 2.
Convergence history in the Darcy flow regime, $Da = 10^{-6}$, $Ra = 10^{8}$

Note: Solution obtained with zero initial conditions ($u_1 = 0$, $u_2 = 0$, $p = 0$ and $T = 0$)

The average Nusselt numbers calculated from both schemes on both the fine and coarse meshes are presented in Table II. As can be seen, on the fine mesh, the results obtained by both the schemes are very close to the available Darcy flow regime solution (Walker and Homsy, 1978; Lauriat and Prasad, 1989). However, here the *QI* scheme has a slight advantage over the *SI* scheme on accuracy. In the non-Darcy regime both the schemes give results very close to each other on the fine mesh. On the coarse mesh both the schemes give results different from that of the literature values. This can be attributed to the coarseness of the mesh used here.

The second problem considered in this paper is the buoyancy driven flow from a hot circular cylinder buried in a fluid saturated porous medium. Study of this type of problem is useful in the applications of nuclear waste disposal and in crude oil transport (Himasekhar and Bau, 1989; Nithiarasu, 1999). A simplified version of such a problem is shown in Figure 5 (half domain). The finite element mesh is also shown in this figure. The total domain width is 4× the diameter of the cylinder and the height is 8× the diameter of the cylinder. The Rayleigh number is defined based on the diameter of the cylinder. The

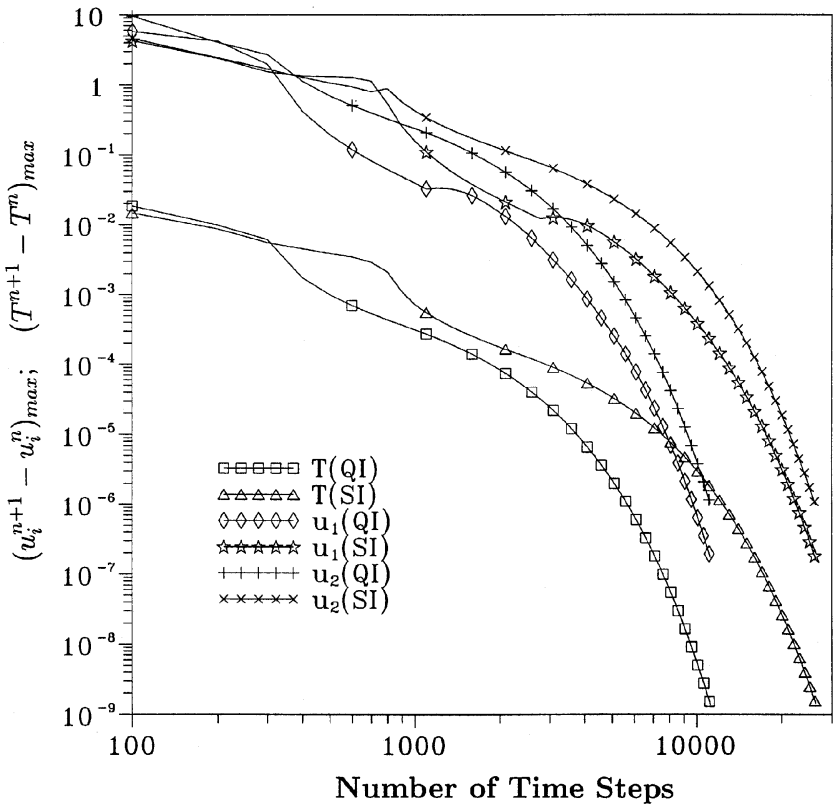

Note: Solution obtained with zero initial conditions ($u_1 = 0$, $u_2 = 0$, $p = 0$ and $T = 0$)

Figure 3.
Convergence history in the Darcy flow regime, $Da = 10^{-6}$, $Ra = 10^9$

cylinder is assumed to be at a higher temperature than that of the outer boundaries. Only one half of the domain is considered (Figure 5 (a)), as symmetry is assumed on the other half of the domain. The velocity components are assumed to be zero on the outer boundaries and on the cylinder surface. The mesh used is fine along the boundaries and also fine near the cylinder surface. In total 3,003 nodes and 5,776 elements are used. Flow and heat transfer in two different flow regimes (Darcy and non-Darcy) and different Rayleigh numbers have been studied.

Before going into quantitative comparison, the performance of the schemes on predicting the flow and heat transfer patterns is compared at various Rayleigh and Darcy numbers. Figure 6 shows the streamlines and isotherms in the Darcy flow regime ($Da = 10^{-6}$) and at $Ra = 10^8$. As can be seen, the results of both schemes are in excellent agreement with each other. Even the maximum stream function values are very close to each other. Although small differences in the isotherm patterns are noticed, in general the flow and isotherm patterns of the schemes match well.

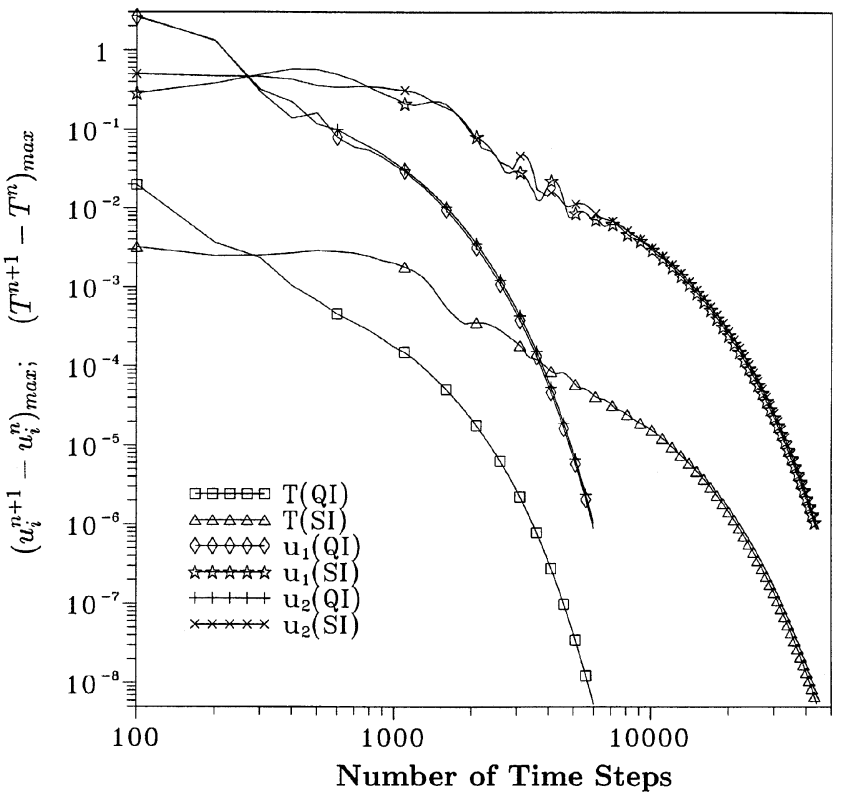

Figure 4.
Convergence history in the non-Darcy flow regime, $Da = 10^{-2}$, $Ra = 5 \times 10^5$

Note: Solution obtained with zero initial conditions ($u_1 = 0$, $u_2 = 0$, $p = 0$ and $T = 0$)

Table II.
Comparison of average Nusselt number (Nu): buoyancy driven flow in a square cavity

Da	*Ra*	*SI* (Fine grid)	*QI* (Fine grid)	*SI* (Coarse grid)	*QI* (Coarse grid)	Walker & Homsy (1978)	Lauriat & Prasad (1989)
10^{-6}	10^8	2.99	3.012	2.664	2.884	3.097	3.09
10^{-6}	10^9	12.435	12.856	10.478	12.932	12.96	13.41
10^{-6}	5×10^9	29.60	32.364	20.603	not converged	–	–
10^{-2}	10^4	1.537	1.554	1.524	1.554	–	–
10^{-2}	10^5	3.608	3.607	3.554	3.566	–	–
10^{-2}	5×10^5	6.042	6.037	6.069	6.118	–	–

Figures 7 and 8 show the transient flow and isotherm patterns with respect to time for the quasi- and semi-implicit schemes respectively. There is experimental evidence in the literature of this type of transient development at higher Rayleigh numbers (Himasekhar and Bau, 1989). This is due to the

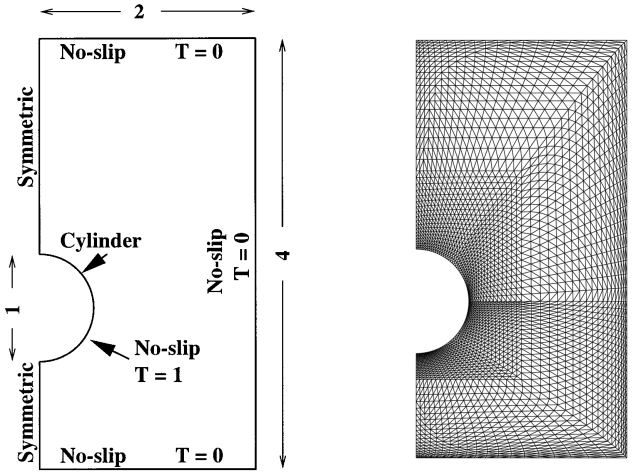

(a) Geometry and boundary conditions

(b) Finite element mesh, Nodes: 3,003, Elements: 5,776

Figure 5.
Buoyancy driven flow from a cylinder buried into a fluid saturated porous medium

instability developed as a result of the increase in the Rayleigh number and results in plumes rising from the cylinder. Although the flow and isothermal pattern continuously changed with respect to time and developed a cyclic pattern, this has not influenced much the overall heat transfer, as can be seen later. Thus the transient patterns obtained here are very mild. There are some differences between the schemes in the flow and isotherm patterns, especially in the shape of the eye of the vortices and in isotherm patterns near the top boundary. Even with these changes the maximum values of stream function seem to be close for both the schemes and also with respect to time.

Figure 9 shows the steady state streamlines and isotherms in the non-Darcy regime ($Da = 10^{-2}$) at $Ra = 5 \times 10^4$. Although the patterns agree in general, a careful investigation shows differences in the shape of the eye of the vortices. Also the isotherm patterns differ considerably in the area above the cylinder. A marginal difference in the values of the maximum stream function is also observed here. If we assume that the results obtained by the quasi-implicit form are more accurate than that of the semi-implicit scheme, the semi-implicit scheme gives the effect of a smaller Rayleigh number than that of the given Rayleigh number and vice versa.

The real huge difference is obtained in the non-Darcy regime at a Rayleigh number of 10^5, as is shown in Figures 10 and 11. While the quasi-implicit scheme predicted a transient heat transfer mechanism, the semi-implicit form has given a steady solution. The quasi-implicit scheme gives a solution which has no steady state but varies with time in a cyclic fashion. In Figure 10, two different flow and isotherm patterns from this cycle are given at two different

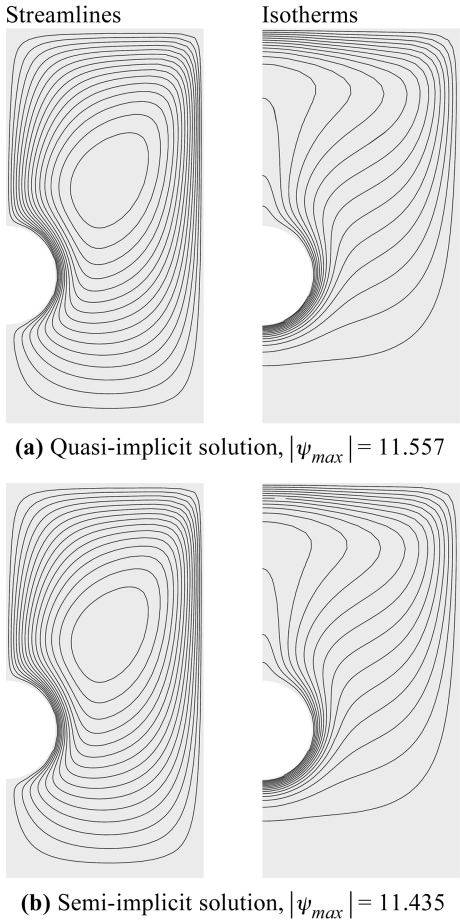

Note: Flow and isotherm patterns at Ra = 10^8, Da = 10^{-6}, $\varepsilon = 0.5$

Figure 6.
Buoyancy driven flow from a cylinder buried in a fluid saturated porous medium

non-dimensional times. Figure 11 shows the steady solution given by the semi-implicit form for the same Darcy and Rayleigh numbers.

As can be seen from the steady state results of Figure 9, the results of Figures 10 and 11 again confirm the conclusion that either the semi-implicit scheme gives an effect of a smaller Rayleigh number than that of the given one or the quasi-implicit scheme gives the effect of a higher Rayleigh number. From the comparison of converged results of the first problem considered in this paper with other results and also from the fact that the transient terms are treated properly in the quasi-implicit scheme, one can conclude that the quasi-implicit schemes are more accurate than the semi-implicit scheme.

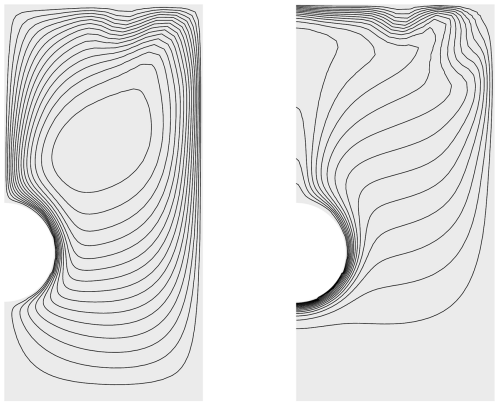

(a) t = 1.69, $|\psi_{max}|$ = 17.699

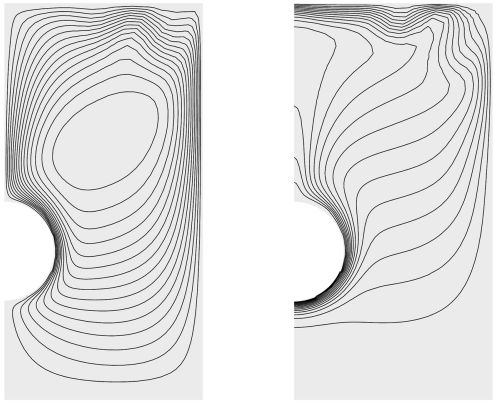

(b) t = 2.02, $|\psi_{max}|$ = 17.777

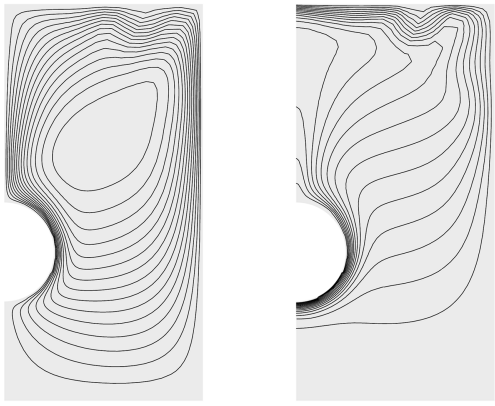

(c) t = 2.57, $|\psi_{max}|$ = 17.771

Note: Transient flow and isotherm patterns at Ra = 2×10^8, Da = 10^{-6}, $\varepsilon = 0.5$. Quasi-implicit solution

Figure 7.
Buoyancy driven flow from a cylinder buried in a fluid saturated porous medium

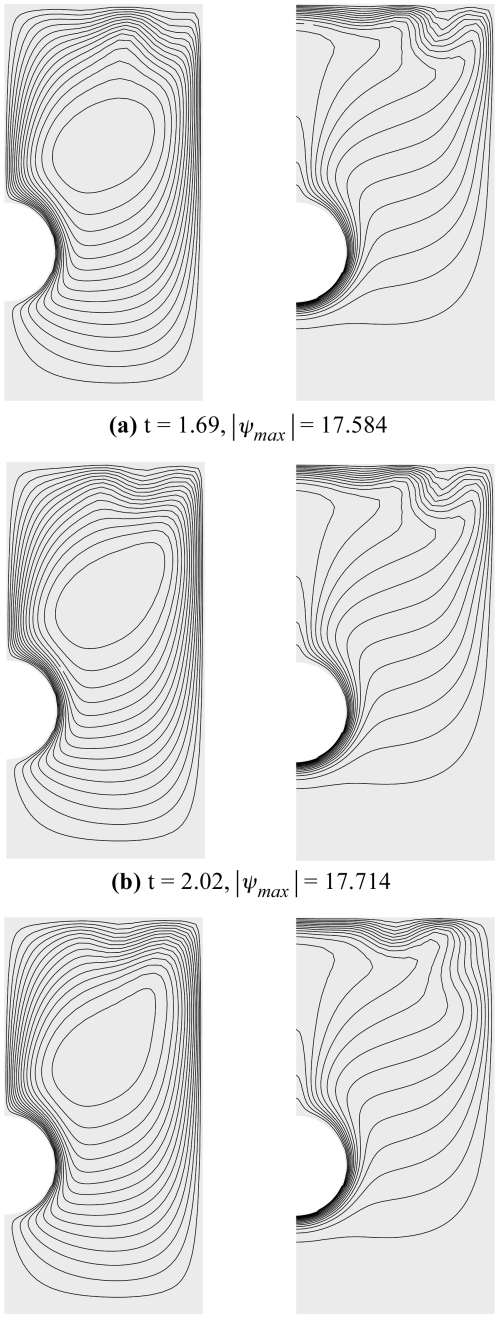

(a) t = 1.69, $|\psi_{max}|$ = 17.584

(b) t = 2.02, $|\psi_{max}|$ = 17.714

(c) t = 2.57, $|\psi_{max}|$ = 17.571

Note: Transient flow and isotherm patterns at Ra = 2×10^8, Da = 10^{-6}, $\varepsilon = 0.5$. Semi-implicit solution

Figure 8.
Buoyancy driven flow from a cylinder buried in a fluid saturated porous medium

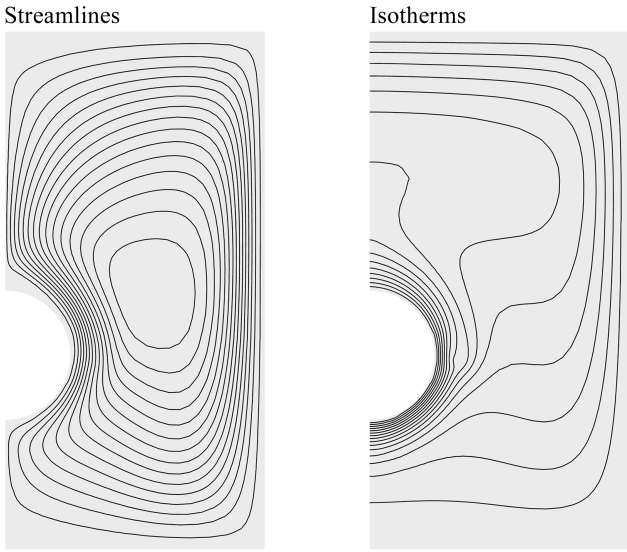

(a) Quasi-implicit solution, $|\psi_{max}| = 18.954$

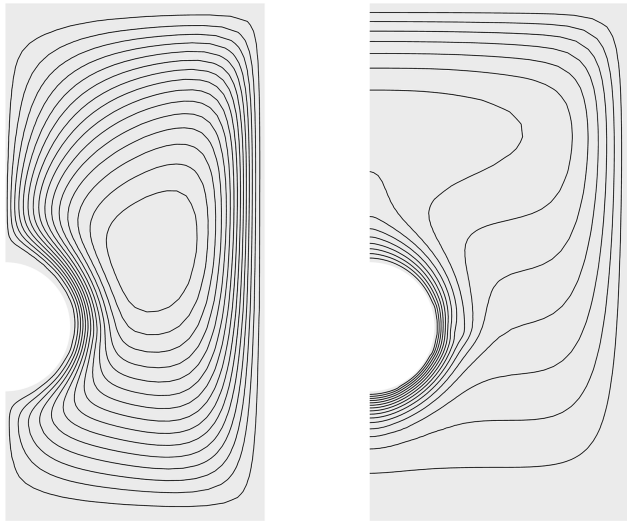

(b) Semi-implicit solution, $|\psi_{max}| = 15.103$

Note: Flow and isotherm patterns at $Ra = 5 \times 10^4$, $Da = 10^{-2}$, $\varepsilon = 0.5$

Figure 9.
Buoyancy driven flow from a cylinder buried in a fluid saturated porous medium

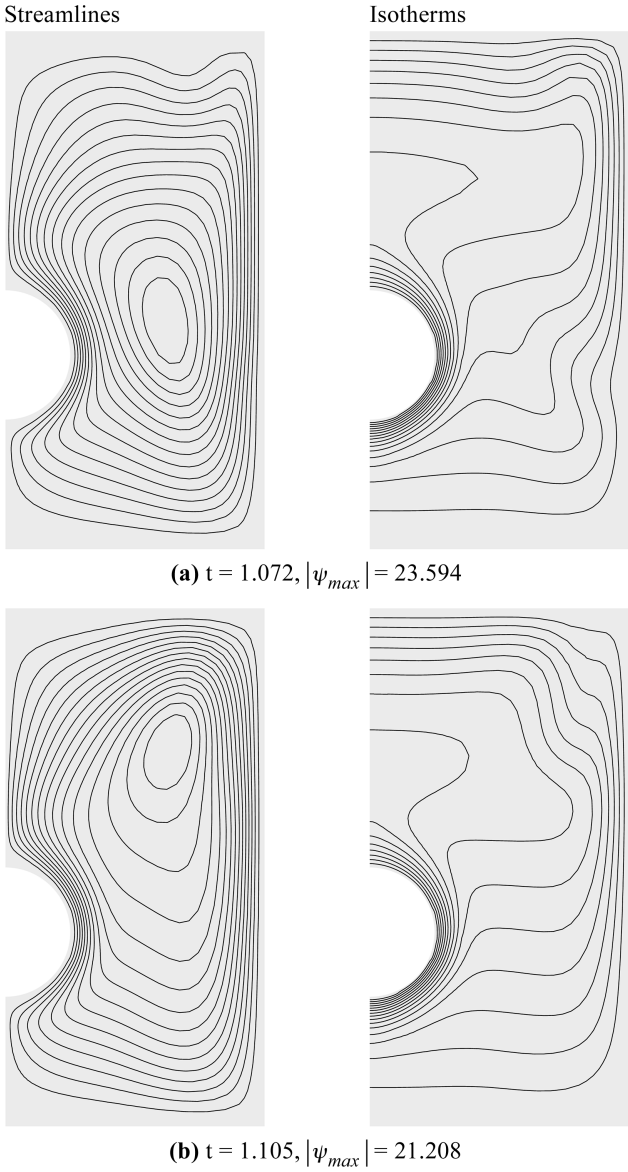

Figure 10.
Buoyancy driven flow from a cylinder buried in a fluid saturated porous medium

Note: Transient flow and isotherm patterns at Ra = 10^5, Da = 10^{-2}, $\varepsilon = 0.5$. Quasi-implicit solution

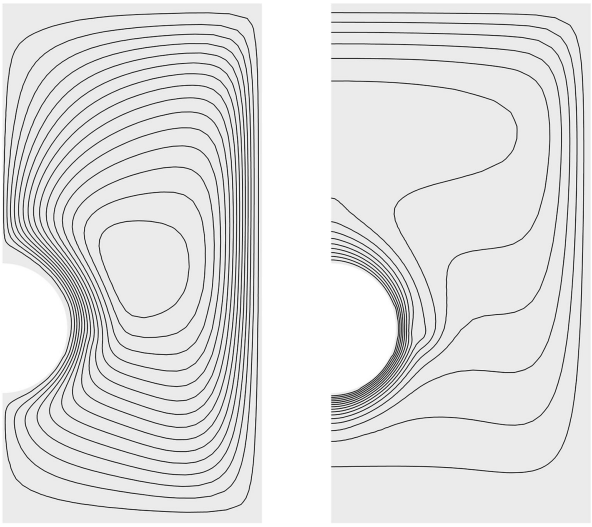

Note: Flow and isotherm patterns at Ra = 10^5, Da = 10^{-2}, $\varepsilon = 0.5$. Semi-implicit solution, $|\psi_{max}| = 21.244$

Figure 11.
Buoyancy driven flow from a cylinder buried in a fluid saturated porous medium

Da	*Ra*	*SI*	*QI*
10^{-6}	10^7	29,667 (3×10^{-5})	716 1×10^{-2}
10^{-6}	5×10^7	28,467 (3×10^{-5})	1,069 5×10^{-3}
10^{-6}	10^8	24,674 (3×10^{-5})	5,643 7×10^{-4}
10^{-6}	2×10^8	transient	transient
10^{-2}	10^3	26,251 (3×10^{-5})	713 1×10^{-2}
10^{-2}	5×10^3	35,193 (3×10^{-5})	1,339 5×10^{-3}
10^{-2}	2×10^4	40,055 (3×10^{-5})	60,134 1×10^{-4}
10^{-2}	5×10^4	46,168 (3×10^{-5})	127,722 5×10^{-5}
10^{-2}	10^5	49,955 (3×10^{-5})	transient –

Note: The time steps used in each case are given in parentheses

Table III.
Comparison of CPU time in seconds on a Pentium 166 for the buried cylinder problem

Table III shows the CPU time taken by each scheme and the time steps used in each case. The CPU comparison is similar to the first problem studied in this paper on a fine mesh. At smaller Rayleigh numbers again the *QI* scheme has the advantage of efficiency over the *SI* scheme. However, at higher Rayleigh numbers, in the non-Darcy regime, the *SI* scheme is more efficient than that of the *QI* scheme. The solution was not obtained beyond $Ra = 2 \times 10^8$ in the Darcy flow regime nor beyond 10^5 in the non-Darcy flow regime, as the flow turned into a transient state beyond these limits.

In Table IV, the average Nusselt numbers obtained on the buried cylinder problem are compared for both the schemes. In general the average Nusselt number predicted by the *SI* scheme are equal to or smaller than that of the *QI* scheme except for $Ra = 10^5$ in the non-Darcy flow regime, where the average Nusselt number predicted by the *SI* scheme is higher than that of the *QI* scheme. This change in trend can be attributed to the transient developments occurring when the *QI* scheme was used at $Ra = 10^5$ in the non-Darcy flow regime. The average Nusselt number given for the *QI* scheme at $Ra = 10^5$ is time averaged over a transient cycle.

5. Conclusions

A comparative study has been carried out to evaluate the performance of two different time stepping schemes for natural convection in a fluid saturated porous medium. Both the schemes were tested on two different problems. Although the *QI* scheme is faster at lower Rayleigh numbers, the *SI* scheme has the advantage of speed at higher Rayleigh numbers, especially in the Darcy flow regime. On the coarse mesh used, the *SI* scheme has the clear advantage of efficiency over that of the *QI* scheme.

Another point of practical interest is that the *QI* scheme can be used to calculate transients accurately without any further modifications to the code but the *SI* scheme needs modifications. However, features such as the simplicity of the *SI* scheme and its CPU advantages over the *QI* scheme in some flow regimes even on a fine mesh are worth noting.

Table IV. Comparison of average Nusselt number (Nu) for the buried cylinder problem

Da	*Ra*	*SI*	*QI*
10^{-6}	10^7	1.182	1.184
10^{-6}	5×10^7	2.373	2.430
10^{-6}	10^8	3.517	3.673
10^{-6}	2×10^8	5.419	5.722
10^{-2}	10^3	1.173	1.133
10^{-2}	5×10^3	1.568	1.651
10^{-2}	2×10^4	2.249	2.387
10^{-2}	5×10^4	2.893	3.024
10^{-2}	10^5	3.526	3.089 (transient)

References

Chorin, A.J. (1968), "Numerical solution of Navier-Stokes equations", *Math. Comp.*, Vol. 22, pp. 745-62.

Comini, G. and Del Giudice, S. (1982), "Finite element solution of incompressible Navier-Stokes equations", *Num. Heat Transfer, Part A*, Vol. 5, pp. 463-78.

Donea, J., Giuliani, S., Laval, H. and Quartapelle, L. (1982), "Finite element solution of unsteady Navier-Stokes equations by a fractional step method", *Comp. Meth. Appl. Mech. Eng.*, Vol. 33, pp. 53-73.

Ergun, S. (1952), "Fluid flow through packed column", *Chemical Engineering Progress*, Vol. 48, pp. 89-94.

Gartling, D.K., Hickox, C.E. and Givler, R.C. (1996), "Simulation of coupled viscous and porous flow problems", *Comp. Fluid. Dyn.*, Vol. 7, pp. 23-48.

Hickox, C.E. and Gartling, D.K. (1985), "A numerical study of natural convection in a vertical porous layer", *Int. J. Heat Mass Transfer*, Vol. 28, pp. 720-23.

Himasekhar, K. and Bau, H.H. (1989), "Thermal convection around a heat source embedded in a box containing a saturated porous medium", *ASME J. Heat Transfer*, Vol. 110, pp. 649-54.

Hsu, C.T. and Cheng, P. (1990), "Thermal dispersion in a porous medium", *Int. J. Heat Mass Transfer*, Vol. 33, pp. 1587-97.

Lauriat, G. and Prasad, V. (1989), "Non-Darcian effects on natural convection in a vertical porous enclosure", *Int. J. Heat Mass Transfer*, Vol. 32, pp. 2135-48.

Massarotti, N., Nithiarasu, P. and Zienkiewicz, O.C. (2000), "Porous-fluid interface problems. A characteristic based split (CBS) procedure", *ECCOMAS 2000*, Barcelona, 11-14 September.

Misra, D. and Sarkar, A. (1995), "A comparative study of porous media models in a differentially heated square cavity using finite element method", *Int. J. Num. Meth. Heat & Fluid Flow*, Vol. 5, pp. 735-52.

Nishimura, T., Takumi, T., Shiraishi, M., Kawamura, Y. and Ozoe, H. (1986), "Numerical analysis of natural convection in a rectangular enclosure horizontally divided into fluid and porous regions", *Int. J. Heat Mass Transfer*, Vol. 29, pp. 889-98.

Nithiarasu, P. (1999), "Finite element modelling of migration of a third component leakage from a heat source buried in a fluid saturated porous medium", *Mathematical and Computer Modelling*, Vol. 29 No. 4, pp. 27-39.

Nithiarasu, P. and Ravindran, K. (1998), "A new semi-implicit time stepping procedure for buoyancy driven flow in a fluid saturated porous medium", *Comp. Meth. Appl. Mech. Eng.*, Vol. 165, pp. 147-54.

Nithiarasu, P., Seetharamu, K.N. and Sundararajan, T. (1996), "Double-diffusive natural convection in an enclosure filled with fluid saturated porous medium – a generalised non-Darcy approach", *Numerical Heat Transfer, Part A*, Vol. 30, pp. 413-26.

Nithiarasu, P., Seetharamu, K.N. and Sundararajan, T. (1997), "Natural convective heat transfer in an enclosure filled with fluid saturated variable porosity medium", *Int. J. Heat Mass Transfer*, Vol. 40 No. 16, pp. 3955-67.

Nithiarasu, P., Seetharamu, K.N. and Sundararajan, T. (1998a), "Effects of porosity on natural convective heat transfer in a fluid saturated porous medium", *Int. J. Heat Fluid Flow*, Vol. 19, pp. 56-8.

Nithiarasu, P., Seetharamu, K.N. and Sundararajan, T. (1998b), "Finite element analysis of pollutant transport in water saturated soil", *Comm. Num. Meth. Eng.*, Vol. 14, pp. 241-51.

Nithiarasu, P., Seetharamu, K.N. and Sundararajan, T. (1999), "Numerical investigation of buoyancy driven flow in a fluid saturated non-Darcian porous medium", *Int. J. Heat Mass Transfer*, Vol. 42, pp. 1205-15.

Nithiarasu, P., Sujatha, K.S., Sundararajan, T. and Seetharamu, K.N. (1999), "Buoyancy driven flow in a non-Darcian fluid - saturated porous enclosure, subjected to uniform heat flux – a numerical study", *Comm. Num. Meth. Eng.*, Vol. 15, pp. 765-76.

Nithiarasu, P., Sujatha, K.S., Ravindran, K., Sundararajan, T. and Seetharamu, K.N. (2000), "Non-Darcy natural convection in a hydrodynamically and thermally anisotropic porous medium", *Comp. Meth. Appl. Mech. Eng.*, Vol. 188, pp. 413-30.

Rajamani, R., Srinivas, C. and Seetharamu, K.N. (1990), "Finite element analysis of convective heat transfer in porous media", *Int. J. Num. Meth. Fluids*, Vol. 7, pp. 331-9.

Rajamani, R., Srinivas, C., Nithiarasu, P. and Seetharamu, K.N. (1995), 'Convective heat transfer in axisymmetric porous bodies", *Int. J. Num. Meth. Heat & Fluid Flow*, Vol. 5 No. 9, pp. 829-37.

Ramaswamy, B. (1988), "Finite element solution for advection and natural convection flows", *Comp. Fluids*, Vol. 16, pp. 349-88.

Ramaswamy, B. (1993), "Theory and implementation of a semi-implicit finite element method for viscous incompressible flows", *Comp. Fluids*, Vol. 22, pp. 725-47.

Ramaswamy, B., Jue, T.C. and Akin, J.E. (1992), "Semi-implicit and explicit finite element schemes for coupled fluid/thermal problems", *Int. J. Num. Meth. Engg.*, Vol. 34, pp. 675-96.

Sai, B.V.K.S., Seetharamu, K.N. and Aswathanarayana, P.A. (1997), "Finite element analysis of heat transfer by natural convection in vertical enclosures: investigations in Darcy and non-Darcy regimes", *Int. J. Num. Meth. Heat & Fluid Flow*, Vol. 7, pp. 367-401.

Vafai, K. and Tien, C.L. (1981), "Boundary and inertia effects on flow and heat transfer in porous media", *Int. J. Heat Mass Transfer*, Vol. 24, pp. 195-203.

Walker, K.L. and Homsy, G.M. (1978), "Convection in porous cavity", *J. Fluid Mech.*, Vol. 87, pp. 449-74.

Zienkiewicz, O.C. and Codina, R. (1995), "A general algorithm for compressible and incompressible flow, Part I: The split characteristic based scheme", *Int. J. Num. Meth. Fluids*, Vol. 20, pp. 869-85.

Zienkiewicz, O.C. and Taylor, R.L. (2000), *The Finite Element Method*, Vol. 1. *Basis*, 5th edition, Butterworth, London.

Zienkiewicz, O.C., Nithiarasu, P., Codina, R., Vázquez, M. and Ortiz, P. (1999), "The characteristic based split procedure. An efficient and accurate algorithm for fluid problems", *Int. J. Num. Meth. Fluids*, Vol. 31, pp. 359-92.